

# Cellular SiC ceramic from stems of corn – processing and microstructure

ANUP K. BHATTACHARYA, JÜRGEN G. HEINRICH\*  
*Institut für Nichtmetallische Werkstoffe, TU Clausthal, Germany*  
*E-mail: heinrich@naw.tu-clausthal.de*

Published online: 9 March 2006

SiC-based cellulosic composites were prepared using maize and barley stems as precursors. Reactive melt infiltration has been chosen as processing method. In spite of very weak and thin cell walls of maize stems, honeycomb microstructure of maize stems was retained by using a slow infiltration technique. Residual silicon could also be removed from the final composite by treating the infiltrated sample under high vacuum and at high temperature viz. 1600°C. Hollow cylindrical SiC composites were obtained from the stems of barley and SiC-cylinders supported by honeycomb SiC core was obtained from the stems of maize. Detailed microstructural features of the pyrolysed and infiltrated maize/barley stems were explored in this work.

© 2006 Springer Science + Business Media, Inc.

## 1. Introduction

Material synthesis from woods and plant stems has recently become an area of increasing interest mainly due to their anisotropic microstructural features. These anisotropic microstructures of woods/plant stems impart some interesting properties to it such as high stiffness and anisotropic permeability. Highly aligned and elongated longitudinal cells in wood are ideally suited for fluid transport in the axial direction. This anisotropic permeability of wood may be exploited for some specific applications. The aligned fibrous cells are also responsible for the high stiffness of the stems. Thus, woods/plant stems are considered as better precursor materials for some specific applications than some regular foam, owing to their anisotropic properties.

Many attempts were made to produce near net-shaped polymer, ceramic and carbon composites from these natural resources. These works were mostly done in two steps:

1. Controlled thermal decomposition (pyrolysis) to form a monolithic carbon template which retains the anatomical features of the precursors.

2. Conversion of these carbon templates into the required composite through infiltrations, either by gas phase or by liquid phase.

Major constituents of wood are cellulose, hemicellulose and lignin. Detailed analysis was performed to understand

the mechanism of pyrolysis of wood materials [1, 2]. It has been suggested that pyrolysis takes place in four steps: (a) desorption of adsorbed water up to 150°C, (b) splitting off of hemicellulose at 200–260°C, (c) depolymerisation of cellulose at 240–350°C, lignin at 280–500°C and (d) aromatisation forming graphitic layers above 400°C.

Controlled pyrolysis can lead to crack free carbon templates and it has also been shown that these carbon templates have better strength than the precursor woods [3]. Different types of composites were fabricated from these wood precursors but most of the works concentrated on the formation of SiC-based composites. Oak wood has been converted to cellular SiC ceramic through SiO gas phase reaction of the carbonised Oak wood [4]. Oak has also been converted to Si/SiC composite through melt infiltration into oak charcoal. Three point flexural strength of these composites were reported to be 330 MPa at room temperature and 280 MPa at 1300°C [5]. Microstructure of the wood precursors could also dictate the final properties of the composite. Some studies were performed on the effect of microstructure on the fracture behaviour and other mechanical properties of biomorphous SiC ceramics. Composites with different microstructure could be prepared using different types of woods. Extensive study has been carried out on the liquid infiltration of Si into the carbon templates obtained from Ebony, Beech, Oak, Maple, Pine and Balsa. Mechanical property measurements of these composites were done and some

\*Author to whom all correspondence should be addressed.

microstructure-property relationship was established [6, 7].

Not only melt infiltration of Si or vapour infiltration with SiO helps in getting SiC based composites but some different routes are also available to get these composites. Some highly porous cellular SiC were obtained from pine wood by vapour infiltration of Si, SiO and  $\text{CH}_3\text{SiCl}_3$  into the carbonised template [8]. Ota *et al.* had vacuum infiltrated oak charcoal with tetraethyl ortho silicate (TEOS). TEOS in the cell structure was hydrolysed in an ammoniacal solution to form  $\text{SiO}_2$  gel, which was in turn fired at  $1400^\circ\text{C}$  in argon to form  $\alpha$ -SiC. This method also helps in getting a carbon precursor with various char contents which can in turn be converted to SiC. Thus density can also be tailored in the final composite [9]. In this work, stems of barley and maize have been chosen as precursor materials. These materials were specifically chosen in order to produce composites with cylindrical geometry. From barley stems we could only obtain some hollow cylinders, while the scope for production of some cylindrical shell, supported by a honeycomb bulk was possible only from maize stems. In nature, these stems are loaded in some combination of axial compression and bending. Failure in these stems was reported to be typically by buckling [10]. It has been reported that stems with filled foams are mechanically more efficient than their hollow counterparts and they are more resistant to buckling. In this work, SiC-ceramics were produced from the stems of barley and maize. Optimisation of the infiltration conditions and a detailed microstructural analysis has been produced here.

## 2. Experimental

Simultaneous thermal analysis (STA) (NETZSCH 409 PC/PG) of the stems was done in argon atmosphere. Rate of heating was maintained at 10 K/min till  $1000^\circ\text{C}$ . Flow rate of argon was maintained at 50 c.c./min. Samples of 10 mm length were cut by a sharp razor blade from the dried stems for pyrolysis. Pyrolysis was done in an electric furnace (Linn GmbH elektronik VMK22) under flowing nitrogen atmosphere. Heating rate was maintained at 5 K/min till  $300^\circ\text{C}$  followed by 10 K/min till  $800^\circ\text{C}$ . After  $800^\circ\text{C}$ , furnace was slowly cooled at a rate of 10 K/min. Infiltration of these pyrolysed stems was carried out in a gas pressure furnace (KCE, FCT GmbH, Germany). Different techniques were adopted for infiltrations. In the first process, which may be called direct infiltration technique (DIT), preform was kept directly above the infiltrant powder. In the second process, preform and infiltrant powder were connected through a carbon fibre. This process is named as slow infiltration technique (SIT). Silicon powder (Alfa Aesar,  $\sim 325$  mesh, 99.999%) was used as infiltrant. For both the above mentioned processes, entire set up was arranged in BN plates which were then placed into BN crucibles. These were then put into the furnace for infiltration. Infiltrations were performed in argon as well as in vacuum. In the DIT, heating rate was maintained

at 20 K/min. Different infiltration temperatures were used, ranging from  $1400^\circ\text{C}$  to  $1700^\circ\text{C}$ . Infiltrations were also performed for various durations at each temperature (15 min to 1 h). In SIT, furnace was initially heated at a rate of 20 K/min till  $1250^\circ\text{C}$ . After that, the rate was slowed down to 5 K/min till  $1450^\circ\text{C}$ . At  $1450^\circ\text{C}$ , sample was kept for 10 min followed by cooling at the rate of  $-20$  K/min till  $1000^\circ\text{C}$  was reached. After that, furnace was switched off for self cooling. Scanning electron microscope (SEM) (CamScan CS4, Cambridge, U.K) and Light microscope were used for microstructure analysis. Phase analyses were performed by EDX and X-ray diffractometry (PHILIPS, PW1050, Holland). Relative density of the pyrolysed and infiltrated samples were measured using classical stereological method.

## 3. Result and discussion

Thermal gravimetric analyses (TGA) show a mass loss of around 70% in both the samples. This mass loss was due to the evaporation of surface water and release of some gases during the decomposition of cellulose and lignin present in the precursor. From the DTA analyses, an endothermic peak at around  $100^\circ\text{C}$  could be seen in all the samples. This peak may correspond to the vaporisation of surface water. DTA analysis of maize also shows one exothermic peak at around  $300^\circ\text{C}$  and some endothermic peaks at  $489^\circ\text{C}$ ,  $615^\circ\text{C}$  and  $890^\circ\text{C}$ . These peaks may correspond to the depolymerisation of hemicellulose, cellulose and lignin [1, 2]. Detailed analysis of these reactions is beyond the scope of this work. STA graph for maize is shown in Fig. 1.

No cracks were observed in the pyrolysed samples and the honeycomb microstructure of the bulk was found to be replicated in the carbon templates. Honeycomb microstructure was seen in the shell of barley and in the core of maize. No pores or honeycomb were seen in the shell of maize. Percentage shrinkage in the axial and radial directions for both barley and maize stems were found to be  $\sim 18\%$  and  $\sim 27\%$ , respectively. Shrinkage in the radial direction was difficult to measure precisely as the cross section was not a complete circle. Every sample was observed to have a bent directed inside.

### 3.1. Barley

In pyrolysed barley stem, there was no honeycomb core present. However, shell of the pyrolysed barley stem retained a honeycomb microstructure. Fig. 2a shows the SEM micrograph of pyrolysed barley stem. Parenchyma cells in the Epidermis and Sclerenchyma cells of the hypodermis could be seen. Cell wall thickness of the Sclerenchyma cells was  $\sim 2 \mu\text{m}$  and that of the parenchyma cells were  $\sim 0.5 \mu\text{m}$ . Parenchyma cells were also found enclosed by the hypodermis. These parenchyma cells constitute the major volume of the shell of barley. Parenchyma cells were present in different size from  $25 \mu\text{m}$  to  $40 \mu\text{m}$  in diameter. How-

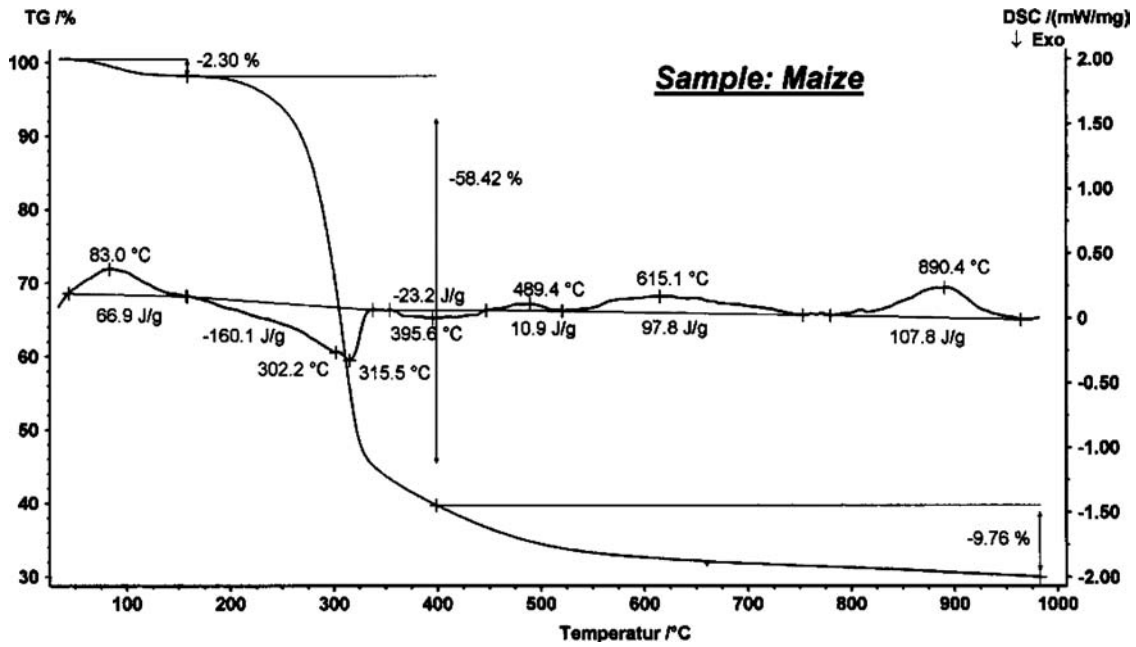


Figure 1 STA Graph for maize stems.

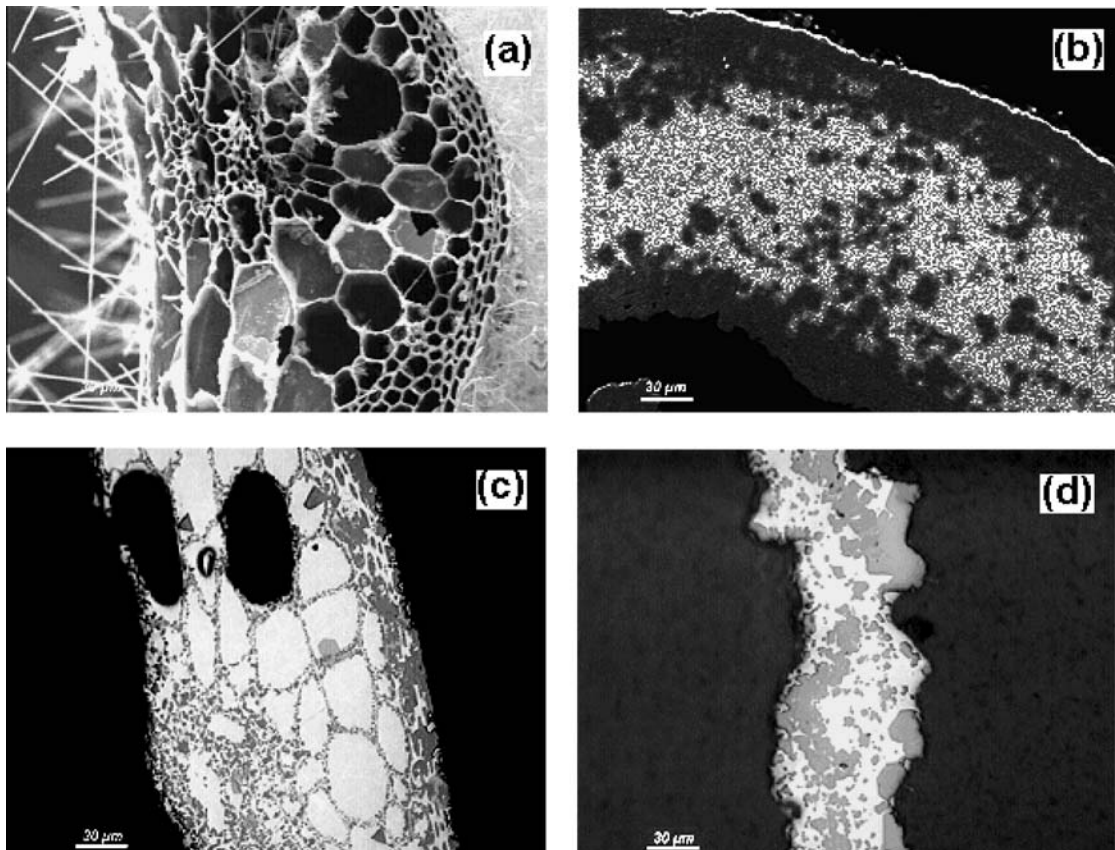


Figure 2 (a) SEM micrograph of pyrolysed barley stem, (b) SEM micrograph of directly infiltrated barley stems at 1450°C, (c) Light microscopic image of infiltrated barley stem at 1450°C by SIT and (d) light microscopic image of re-treated barley stem at 1600°C.

ever, sclerenchyma cells were relatively smaller, around 3  $\mu\text{m}$  in diameter. Some vascular bundles could also be seen in the micrograph consisting of two metaxylem vessels and one protoxylem cavity. Using DIT, at 1450°C, a 10 mm sample was completely infiltrated in 15 min

under a vacuum of 100 Pa. However, no infiltration was observed under argon atmosphere. Silicon doesn't wet the surface of the pyrolysed stem in argon atmosphere. A hollow ceramic tube was obtained upon infiltration. Honeycomb microstructure was not seen in the infiltrated

TABLE I. Comparison of dimensions of cell, cell size and relative density of pyrolysed and infiltrated barley stems. \*SC-Sclerenchyma cell and PC- parenchyma cell

Barley	Cell size ( $\mu\text{m}$ )	Cell wall thickness ( $\mu\text{m}$ )	Relative density
Pyrolysed	$\sim 25\text{--}40$ (PC), $\sim 3$ (SC)	$\sim 2$ (SC), $\sim 0.5$ (PC)	0.4
Infiltrated	$\sim 20\text{--}50$ (PC), $\sim 2$ (SC)	$\sim 6\text{--}4$ (SC), $\sim 1$ (PC)	0.8

sample. Fig. 2b shows the SEM micrograph of infiltrated barley stem at  $1450^\circ\text{C}$  by DIT. All the pores were filled with Si and the final microstructure looks like a composite where SiC is well distributed in a silicon matrix. Dark gray regions are SiC and bright region is Si. Outer and inner layer of the cylindrical shell was mainly composed of SiC. Si was found in between these layers. Silicon might have infiltrated through the walls and through the longitudinal pores present in the pyrolysed preform. In the process, it reacts with the carbon to form  $\beta\text{-SiC}$ . As the carbon precursor was kept directly above the infiltrant, too much melt got access to the honeycomb cells. These excess melt dissolves the carbon template into it and hence no honeycomb microstructure was found in the final composite. X-ray diffraction pattern also reveals the presence of  $\beta\text{-SiC}$  and Si in the composite. However, the honeycomb microstructure was retained in the infiltrated composite, when infiltration was done using SIT. Fig. 2c shows the light microscopic image of slowly infiltrated barley. Dark gray regions are SiC and the bright phase represents silicon. It can be seen that most of the pores are filled with silicon. Upon retreatment of this infiltrated sample at  $1600^\circ\text{C}$  for 30 min, honeycomb microstructure was destroyed. It is assumed that SiC particles, forming the wall get redistributed in the silicon melt. SiC particles distributed in the Si matrix could be seen in the SEM micrograph of retreated sample Fig. 2d. Dark gray particles are SiC and the bright region is Si. Thus, SIT at  $1450^\circ\text{C}$  helps in getting a SiC-Si composite where the honeycomb microstructure of the precursor was retained. Dimensions of the cell size, cell wall and relative density of pyrolysed and infiltrated barley are tabulated in Table I.

### 3.2. Maize

In maize, the shell looks completely solid and the parenchyma or sclerenchyma cells are not seen in the SEM micrograph of the pyrolysed maize Fig. 3a Vascular bundles can be seen well distributed in the core and are supported by parenchyma cells. Parenchyma cells appear as honeycomb network in the core. Density of the vascular bundles was more in the shell as compared to that in the core. These vascular bundles were denser in the shell than in the core. Shell thickness of maize was found to be  $\sim 600\ \mu\text{m}$ . Cells present in the honeycomb core have almost same size of diameter of  $\sim 70\ \mu\text{m}$ . Wall thickness of the cells was  $\sim 8\ \mu\text{m}$ . Vascular bundles present in the honey comb core have a diameter of  $\sim 250\ \mu\text{m}$ ,

TABLE II Comparison of dimensions of cell, cell size and relative density of pyrolysed and infiltrated maize stems

Maize	Cell size ( $\mu\text{m}$ )	Cell wall ( $\mu\text{m}$ )	Relative density
pyrolysed	70	8	0.6
Infiltrated	65	15	0.7

however those which are present in the shell are thinner of  $\sim 170\ \mu\text{m}$  diameter.

Inner core of the maize stem was completely dissolved by the Si melt when preform was kept directly over the infiltrant powder (DIT). Silicon melts at  $1410^\circ\text{C}$  and starts infiltrating through the longitudinal cells present in the core and in the shell. Wall thickness of the cells was so small ( $\sim 8\ \mu\text{m}$ ) that the wall get dissolved into the Si melt during the process. However, by SIT, honeycomb microstructure of the core was retained in the infiltrated composite. 10 mm sample was completely infiltrated at  $1450^\circ\text{C}$  in 10 min. During SIT, Si melts at  $1410^\circ\text{C}$ , slowly approaches the outer wall of the preform and infiltrates through the longitudinal cells present in the shell of maize stem. Si gets diffused through the entire honeycomb network slowly. During diffusion it reacts with the cell walls, forming  $\beta\text{-SiC}$ . In this process, honeycomb network was not destroyed as it allows very limited silicon to slowly diffuse through the cell walls. SEM micrograph of the infiltrated maize is shown in Figs. 3c and d. Upon infiltration, cell wall thickness increases to  $\sim 15\ \mu\text{m}$  from  $8\ \mu\text{m}$  as the wall get converted into  $\beta\text{-SiC}$  from C. Cell size, wall thickness and the relative density of the pyrolysed and infiltrated maize are tabulated in Table II.

Fig. 3c shows the presence of well distributed elongated fibres in the honeycomb core of maize stem. These are the vascular bundles which get detached from the parenchyma cells upon infiltration, hence become more prominent. The shell was also entirely made up of these fibers. Fig. 3c also reveals the higher density of vascular bundles in the shell than that in the core. All these fibers/vascular bundles look porous. Metaxylem and protoxylem vessels of vascular bundles get ruptured, which gives the image of these vascular bundles as hollow fibers. Fig. 3d shows the granular SiC particles in the cell walls. Grain size of SiC particles were in the range of 7 to 11  $\mu\text{m}$ . Si melt could also be found in the middle of these cell walls as the dark gray phase.

Presence of the vessels in the vascular bundles was revealed by the light microscopic image of directly infiltrated maize (Fig. 4). It shows that each of these fibres consist of four hollow cells. Two of them are metaxylem cells, one is protoxylem cavity and the fourth one might have appeared from the rupture of Phloem that was present in between the metaxylem vessels in the direction of cuticle (shell). Hollow vessels are however filled with Si, giving a flowery microstructure. Fig. 4 also reveals that Si got infiltrated into the parenchymatic cells present in the shell of maize and flow of excess Si breaks many of these cell walls. Density of SiC (dark gray phase) was found to be more near the vascular bundles. These might

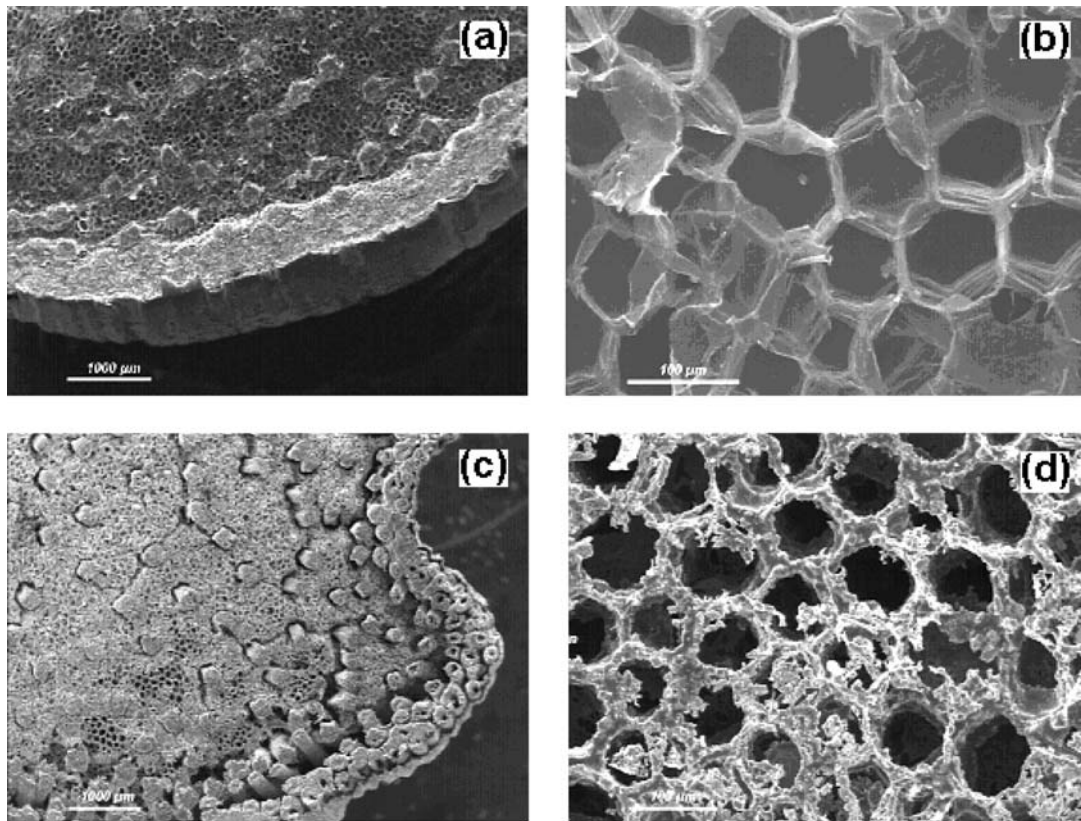


Figure 3 (a) & (b) SEM micrographs of pyrolysed maize stem, (c) & (d) SEM micrographs of infiltrated maize by SIT.

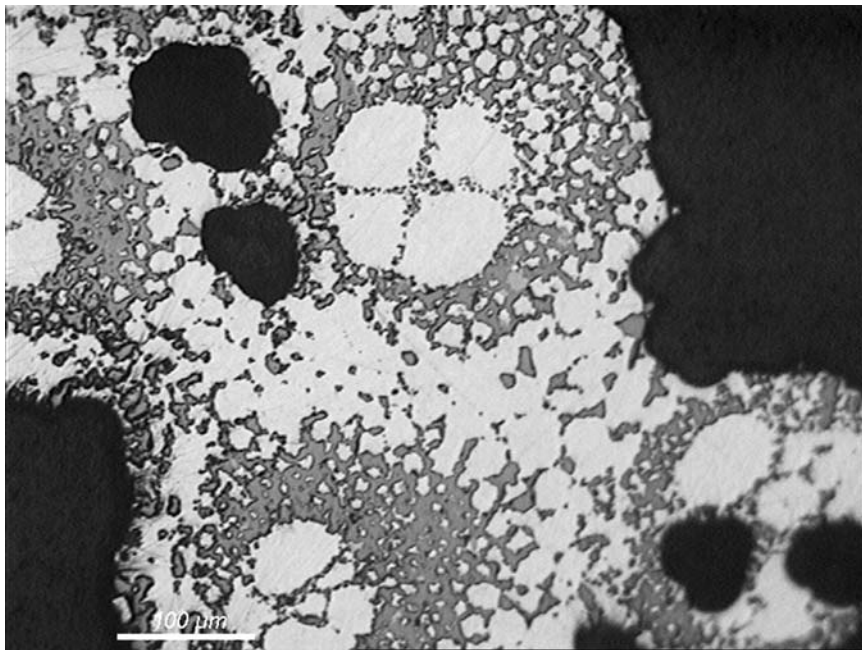


Figure 4 Light microscopic image of the shell of the directly infiltrated maize stem.

have evolved from the dense sheath around the vascular bundles which was present in the raw/pyrolysed maize. This micrograph also proves the presence of epidermis, hypodermis and parenchyma cell in the shell of maize which were not observed in the just pyrolysed maize.

When these infiltrated maize were retreated at 1600°C for 15 min under a vacuum of around 10 Pa, silicon present in the cells get evaporated and no residual silicon was found in the retreated sample. X-ray diffraction pattern of infiltrated maize by SIT at 1450°C and retreated sample

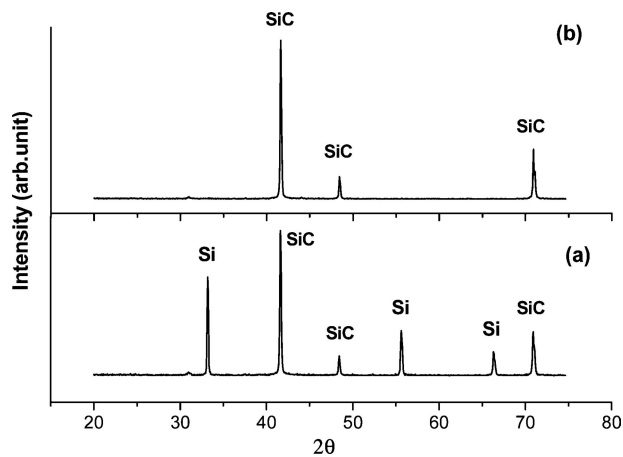


Figure 5 X-ray diffraction pattern of (a) infiltrated maize stem by SIT at 1450°C and (b) re-treated composite at 1600°C.

(at 1600°C) is shown in Fig. 5. No silicon peak was observed in the diffraction pattern of re-treated maize.

#### 4. Conclusion

In spite of the very thin cell wall, successful infiltration of maize and barley stems could be done through a slow infiltration technique. This technique helps in retaining the unique microstructural features of barley and maize. Fine histological structure of barley and maize stems were copied into the final composite through this slow infiltration technique. This technique is much easier and economical as compared to the vapour infiltration techniques, which are usually adopted whenever the cell walls are of such micron range ( $\sim 8 \mu\text{m}$ ). Maize stems show some unique microstructural features which become more prominent upon infiltration. These unique microstructural features of maize stems can be exploited for some specific applications. Work is going on for the selective infiltration of the elongated fibres that are present

in maize stems. This will help in getting some composite which will be equivalent to a fibre reinforced composite, where elongated fibres will be embedded into a honeycomb matrix. This process will also help us in getting composites, where fibres and the matrix will have different composition and we can vary these compositions to develop some composite for some specific application. Work is also in progress for getting a homogeneously distributed composite of  $\text{MoSi}_2$ -SiC from these stems. Complete microstructural analysis and mechanical properties of these composites will be provided in our next communication.

#### Acknowledgment

We would like to thank DAAD for providing financial support to A.K.B for carrying out research in TU Clausthal, Germany. Our sincere thanks also go to Mr. R.Goerke who helped us a lot with SEM and light microscope.

#### References

1. M. TANG and R. BACON, *Carbon* **2** (1964) 211.
2. E. SOLTES and T. ELDER, "Pyrolysis, in Organic chemicals from Biomass" (CRC press, Boca Raton, FL, 1981).
3. C. E. BYRNE and D. C. NAGLE, *Carbon* **35** (2) (1997), 259.
4. E. VOGLI, J. MUKERJI, C. HOFFMAN, R. KLADNY, H. SIEBER and P. GREIL, *J. Am. Ceram. Soc.* **84** (6) (2001) 1236.
5. D. W. SHIN and S. S. PARK, (1999) 2251.
6. P. GREIL, T. LIFKA and A. KAINDL, *ibid. J. Eur. Ceram. Soc.* **18** (1998) 1961.
7. *Idem.* **18** (1998) 1975.
8. P. GREIL, E. VOGLI, T. FEY, A. BEZOLD, N. POPOVSKA, H. GERHARD and H. SIEBER, *ibid.* **22** (2002) p. 2697.
9. T. OTA, M. TAKAHASHI, T. HIBI, M. OZAWA and H. SUZUKI, *J. Am. Ceram. Soc.* **75** (1995) 3409.
10. G. N. KARAM and L. J. GIBSON, *Mat. Sci. Eng.* **C2** (1994) p.113.

Received 28 June 2004  
and accepted 7 July 2005